Large-area Low-cost Substrate Compatible CNT Schottky Diode for THz Detection

Xianbo Yang and Prem Chahal
Terahertz Systems Lab (TeSLa)
Department of Electrical and Computer Engineering,
Michigan State University
2120 Engineering Building, Michigan State University, East Lansing, MI, 48824
yangxian@msu.edu, chahal@egr.msu.edu

Abstract

In this paper, a novel process is developed for the fabrication of CNT Schottky diodes that is simple to implement and large area compatible. The process utilizes an undercut and self-alignment approach for the fabrication of devices having short lengths (< 1 μm). Furthermore, many CNTs assembled in parallel are utilized in the fabrication of devices to attain good impedance matching. Details of THz detector NEP calculation, fabrication and test of diode devices after integration on a plastic substrate are presented. Measured I-V characteristics and sensitivity at 18 GHz demonstrate that high quality devices can be fabricated using the proposed approach. Preliminary results show that the device can attain NEP values in the range of 50 – 150pW/Hz$^{0.5}$ over a frequency range of 10 GHz – 1THz, respectively.

Introduction

Terahertz (THz) waves lies in the frequency range of 0.3 - 10 THz and research in this spectral region has gained significant interest over the last decade. This is largely because it holds great potential in imaging, spectroscopy, security, drug discovery, environmental monitoring, and medical applications [1]. The smaller wavelength of THz provides capability for higher resolution imaging than other traditional lower frequency techniques, such as microwaves. It is also non-ionizing, making it safer than current X-ray imaging technologies. THz spectroscopy provides sub-surface imaging capabilities due to the transparency of non-metallic materials to THz radiation, providing non-destructive testing for a variety of samples. The application of THz in medical applications, such as the detection of cancerous tumors without having to resort to invasive procedures, will be a significant breakthrough [2]. THz imaging is expected to play a significant role in the near future in many areas. This includes medical imaging to adverse weather landing. Recent application of THz imaging includes body scanners for airport security.

High sensitivity THz detectors are required for THz imaging and sensing. Many device technologies have been developed for different detection schemes [1]. This includes, direct detection, heterodyne detection, bolometer, and others [2-4]. Direct detection is desirable as it requires simple circuits and the overall DC power consumption is very low. Thus low-cost, low-power THz imaging systems can be built using this approach. Desirable characteristics for direct detection, especially for imaging applications, include room temperature operation, low noise equivalent power (NEP), broadband operation and overall low-cost. For a THz imaging array, many diode detectors coupled with antennas are required. In other words, many THz pixels are required to make an imaging array (focal plane array, FPA). The diodes occupy significantly less area on a substrate as compared to an antenna structure (< 1%). Thus, in the fabrication of FPAs, significant real estate is wasted on a semiconductor wafer to the passive elements (antennas). It will be desirable to make a large number of detector diodes on a separate substrate and then micro-assemble these diodes on a low-cost substrate housing large antennas.

Recently, some nanoscale THz detectors such as Carbon nanotube (CNT) quantum dots [2], CNT Schottky diodes [3], and CNT bolometer [4] have been developed by applying carbon nanotubes as the core element for THz detection and showed promising results for sensor applications. However, using the existing approaches, device fabrication is challenging and expensive. These devices require high resolution lithography techniques such as e-beam to attain device lengths less than 1 μm or less. Furthermore, the growths of CNTs or similar devices require substrate that can withstand high temperatures. Lithography and temperature requirements are a bottleneck to large-area low-cost processing. Furthermore, the use of these devices in THz applications has not been thoroughly carried out for CNT based devices. It is the intent of this paper to tackle these challenges.

In order to overcome the above challenges, the processes developed should be low-cost large-area compatible with low-temperature processing. High quality single wall semiconducting CNTs can be grown more easily independent of substrates. Thus, new fabrication processes should utilize these through heterogeneous-like integration in order to achieve circuits and devices having desired properties for a wide range of applications. On these lines, in this paper we have developed processes that allow the fabrication of high sensitivity CNT based detectors integrated on plastic substrates for THz applications.

Background: Direct Detector Noise Equivalent Power

In order to determine the sensitivity of a Schottky diode THz detector, equations are first introduced as follow [5]:

$$NEP = \frac{V_n + V_{1/F}}{\beta_V} \tag{1}$$

$$\beta_V = \frac{\gamma}{2} \frac{R_d\left(1-|\Gamma|^2\right)}{\left(1+R_s/R_d\right)^2\left(1+\left(f/f_{ci}\right)^2\right)} \tag{2}$$

$$f_{ci} \equiv \frac{\left(1+R_s/R_d\right)^{1/2}}{2\pi C_j\left(R_s R_d\right)^{1/2}} \tag{3}$$

$$V_n = \left(4k_b T_B\left(R_s + R_d\right)\right)^{1/2} \tag{4}$$

$$V_{1/F} = \left(\frac{A \times \left(R_s + R_d\right) V_{ds}{}^2}{F}\right)^{1/2} \tag{5}$$

Noise Equivalent Power (NEP) is defined as the detector total noise power in a one Hertz bandwidth and represents the minimum detectable signal power at a unity signal-to-noise ratio. The lower NEP means the effective signal to noise is higher and the sensitivity is higher. According to equation (1), NEP is related to voltage noise $(V_n+V_{1/f})$ and voltage sensitivity β_v. Here V_n and $V_{1/f}$ are thermal noise and flicker noise, respectively, and both can be calculated in terms of series resistance R_s and junction resistance R_d of the diode. The intrinsic frequency or cut-off frequency f_{ci} in equation (3) is the maximum frequency the detector can detect at certain bias conditions. The voltage sensitivity β_v in equation (2), which represents the detected voltage divided by the power absorbed in the diode, is strongly dependent on the curvature coefficient γ, and mismatch losses $(1-|\Gamma|^2)$ between antenna and Schottky diode. The curvature coefficient γ is the measurement of the nonlinearity of the diode current–voltage (I–V) characteristic and is given by the ratio of the second derivative of the diode I–V characteristics to its 1st derivative, in most of the case, $\gamma=q/nk_BT_B$. Where k_B is the Boltzmann Constant, T_B is the temperature, q is the electron charge and n is the ideality factor. The maximum γ for Schottky diode at room temperature is close to 40.

It is important to provide good impedance matching between antenna and the Schottky diode. This can be challenging for broadband detection where the impedance matching has to be maintained over a broad frequency range. The resistance of single-wall semiconducting CNTs can be hundreds of kΩ or even tens of MΩ [3], making it difficult to match to antenna elements. It is clear from the equation that, reducing the effective impedance of CNT Schottky diode helps to improve NEP of the detector. We achieve this by using a novel fabrication process which shortens the CNT effective length (decreasing R_s) and by connecting many CNTs in parallel between the metal contacts of the antenna elements.

Single-wall Semiconducting CNT THz Detectors

Simulation

Simulations of CNT Schottky diode THz detector was carried out using the above equations in order analyze sensitivity as a function of bias and number of CNTs. A simplified structure of CNT Schottky diode THz detector is shown in Figure.1 (a). The variables for calculating NEP and β_v in the equations above should be first determined based on the small signal circuit of the diode in Figure.1 (b). Here the diode is connected with the antenna element and the goal is to minimize reflection coefficient Γ between these two elements. Here, R_s is the series resistance of the CNTs Schottky diode and to the first order it is equal to the semiconducting CNT intrinsic resistance R_{CNT} plus the Ohmic contact resistance R_{Ohmic}:

$$R_s = R_{CNT} + R_{Ohmic} \tag{6}$$

In theory, CNT is a 1D structure and its resistance has been proven to follow quantum mechanics principles, and only ballistic resistance exists for a short CNT [6]. However, CNTs can have defects and impurities which introduce photon scattering and increase the resistance [7]. It is shown that for 3μm long semiconducting CNT, R_{CNT} is around 228kΩ and for 6μm long semiconducting CNT, R_{CNT} is around 420kΩ [8], from which an estimation of resistance for 500nm s-SWNT is around 30kΩ. Ohmic Contact resistance is also varied due to applying different metal for contact and the quality of the contact [9]. The lowest Ohmic contact resistance, per CNT, will be applied for simulation, which is R_{Ohmic}=12.9kΩ for a palladium (Pd) metal contact.

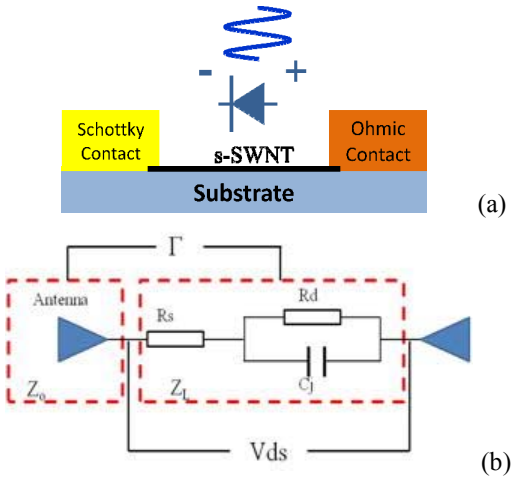

Figure 1. Schottky diode detector (a) and its equivalent model (b)

The junction resistance, R_d, is related to the barrier height at the Schottky contact. Like R_{Ohmic}, R_d will be low for high quality Schottky contacts. In this simulation, we assume the Schottky Contact is perfect and only the barrier height is the dominant factor affecting junction resistance. The junction capacitance C_j of CNTs Schottky Contact represents the electrostatic capacitance plus CNTs unique quantum capacitance. The minimum total junction capacitance measured is ~1aF [8] and can be varying from several aF to 15aF [10]. In our simulation, we choose 1aF for NEP calculations.

There will be power reflected in the circuit due to significant impedance difference between power source (antenna) and the diode. For most of the broadband antennas, the impedance Z_0 ranges from 50Ω (bow-tie antenna) to 180Ω (spiral slot antenna) [16]. By applying equation (7), the reflection coefficient Γ between antenna and the diode can be calculated. Lower value of reflection coefficient is desired to maximize power transferred to the junction of the Schottky diode.

$$\Gamma = \frac{Z_L - Z_o}{Z_L + Z_o} \tag{7}$$

In order to determine the value of R_d and in turn Γ, The I-V Characteristic of CNT Schottky diode was calculated based on information from available literature. Thermionic current (including diffusion current) is the basic part in the total current and can be calculated by the conventional Schottky diode current equation. However, in the CNT Schottky diode, since the carrier concentration is high, the potential barrier is thin such that tunneling current can prevail. The calculation for this tunneling current has been done by several research groups [11] [12]. However, after subscribing necessary values into each current equation, it was determined that the thermionic current dominated the total current. This is

due to the carrier concentration of the CNT used in this research is not very high (effective carrier concentration $N_A \approx 10^{16} cm^{-1}$) and the recombination is strong caused by the small bandgap (≈0.6eV) [13]. Figure 2 shows that the thermionic current is several factors larger than the tunneling current at a lower forward bias, when the ideality factor (n) is 1.5. In some cases, n is around 1.9 [3], which increases the thermionic current. R_d and Γ can be carried out through I-V curve of thermionic current, and the tunneling current is ignored at low forward bias.

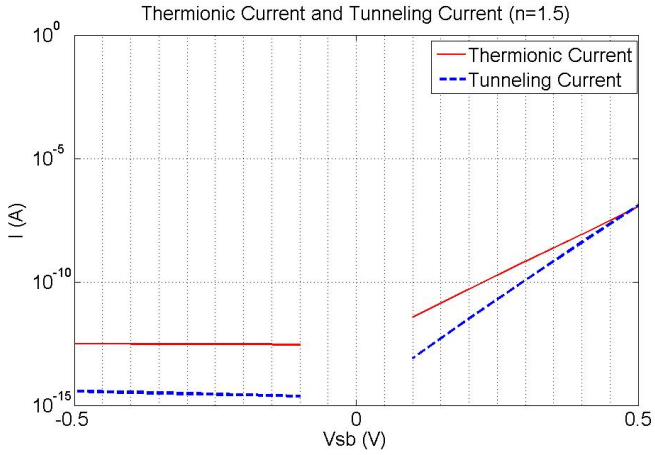

Figure 2. Calculated I-V characteristics of a CNT based Schottky diode.

Simulation Results

The simulation results presented below focus on the NEP value over large bandwidth (1-10THz) and as a function of numbers of CNTs, forward bias, and impedance matching. Figure 3 shows the NEP at 1 THz as a function of bias voltage. It first decrease to $10 pW/Hz^{0.5}$ and then increase above $10^4 pW/Hz^{0.5}$. This shows that an optimum value of forward voltage is required to achieve minimum NEP value. Figure 3 shows simulations under both impedance matching and unmatched conditions.

NEP for Multiple numbers of CNTs connected in parallel between the antenna pads is shown in Figure 4. NEP value decreases when the numbers of CNTs increases. This is largely due to a decrease in R_s and R_d values, which in turn improves sensitivity through improved impedance matching. The NEP value improves from 10 to $1 pW/Hz^{0.5}$ as the number of CNTs connected in parallel increases from 4 to 32, respectively. The NEP value will not continue improving with increase in number of CNTs as the effective capacitance will begin to dominate and the effective impedance will be low. Another negative impact of using very large numbers is that that the CNTs are more likely to entangle with each other and thus become difficult to align. The purity of purchased single-wall semiconducting CNTs batch is around 95% and the remaining are metallic CNTs. Thus there is the risk of having a shorted device when large numbers of CNTs are used.

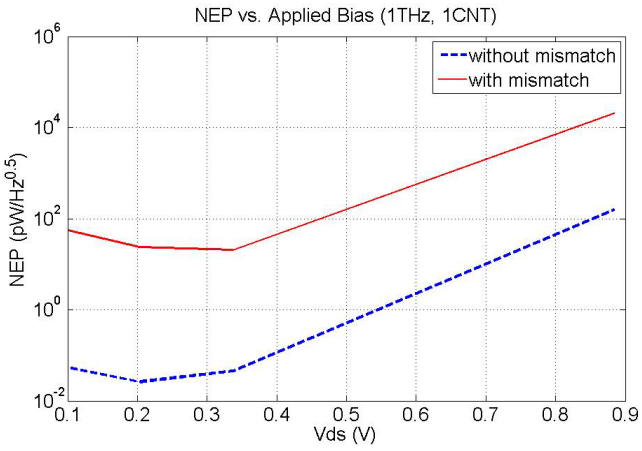

Figure 3. Calculated NEP of a single CNT with and without impedance matching to an antenna element.

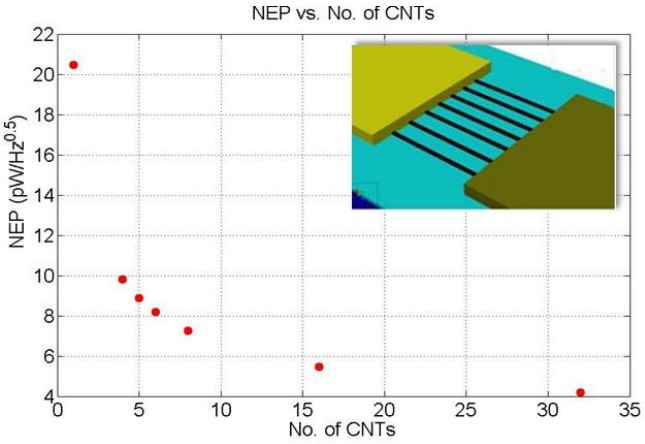

Figure 4. Calculated NEP as a function of CNTs connected in parallel.

Fabrication

Large area low-cost substrates are desirable for THz integration. Among the many large area substrates, polymers based are low cost. Key criterion for selection of substrates, includes: a) low-cost, b) low-loss, wide-band THz characteristics, c) low-dielectric constant, d) high glass transition temperature (> 125 ^oC), and e) process/chemical compatibility, Measured THz characteristics of polymer material show that there are commercially available polymers that can be used for THz applications [14]. Among the many polymers that have low-loss characteristics in THz spectral region, Polyether ether ketone (PEEK), polyimide (PI) and Polyethylene terephthalate (PET) are compatible with chemicals used in the microfabrication processes. Another key requirement is the thermal expansion and the glass transition temperature of the substrate. Table 1 highlights some of the properties for three polymer candidates [15]. Among these three, PET will not be able to withstand some of the process steps. For example, in this research, metal deposition is carried out using e-beam deposition. During the deposition, the temperature on the surface of the substrate can get as high as 100°C and this can build up heat if substrate have low thermal conductivity. Using substrates with higher thermal

conductivity can help in transferring this heat away from the surface. Moreover, thermal expansion is another aspect that should be considered. Thermal mismatch between the different layers can lead to stress build up and leads to warping and cracking. Thus, based on these criterions, PEEK was chosen as the substrate material.

Table 1. Thermal properties of polymer films [15].

	Melting Point °C	Glass Temperature °C	Thermal Expansion K^{-1}	Thermal Conductivity $Wm^{-1}K^{-1}$
PET	>250	75	3.9×10^{-5}	0.15-0.24
PEEK	343	143	2.6×10^{-5}	0.25
Polyimide	N/A	>400	5.5×10^{-5}	0.52

The fabrication process can be divided into three steps: antenna fabrication; CNT alignment; and Schottky and Ohmic contact fabrication. As a first step, Ti metal is deposited which forms as part of the metallization for pads and antenna elements. The importance of this layer is in the alignment of the CNTs. As a second step, the CNTs are aligned through electrophoresis. In the third step, Schottky and Ohmic contacts are formed using a novel self-aligning approach presented in this paper for the first time. Details of these process steps are discussed below.

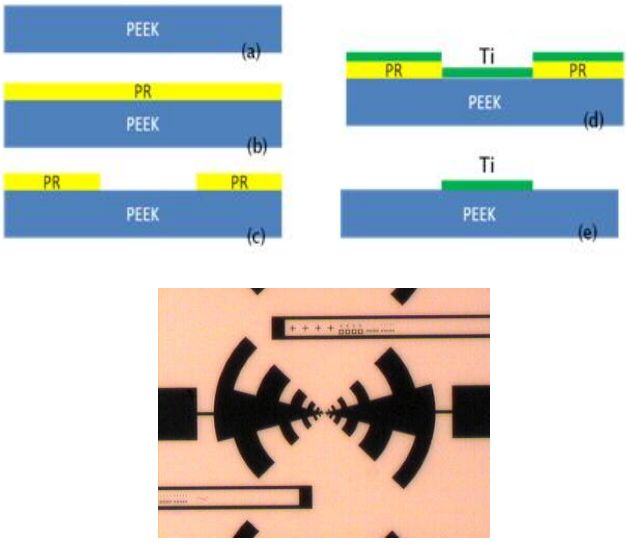

Figure 5. Lift-off of Ti-metal in the fabrication of antenna element (upper) and pads for alignment of CNTs using dielectrophoresis (lower).

Fabrication of Alignment Pads: For the first layer, a broadband log-periodic antenna (LPA) and other metal pads, are fabricated from e-beam deposited 100nm Ti using a lift off process, as shown in Figure 5. For CNT alignment, the gap between the pads was made to be approximately 6 µm. An example fabricated log-periodic antenna from Ti layer is shown in Figure 5. Figure 6 shows the close-up view of the CNT aligning pads at the center of the antenna element. The antenna structure is designed for broad-band signal detection (0.02 – 1 THz) [16].

CNT Alignment: Dielectrophoresis (DEP) is applied in aligning CNTs between the antenna pads, and this is one of the most common approaches implemented in CNT alignment. Theoretical calculations for this can be found in [17]. For this work, a probe station setup was used to probe of the metal pad structures during alignment. An AC source is then applied between metal pads. One droplet of ultrasonicated semiconducting CNTs (NanoIntigris, 2-5µm in length and 1.5-2 nm in diameter) suspended in Iso-propanol alcohol (IPA) is applied between the pads and allowed to dry under the presence of AC field between the pads. In order to achieve good alignment, the conditions such as CNT concentration, ultrasonic time, AC p-p voltage and frequency should be optimized. Multiple CNTs are required for the fabrication of THz detectors. This is beneficial for alignment as multiple CNTs are easier to align than a single CNT.

Figure 6 shows SEM pictures of aligned CNTs from different concentration of CNT suspension in IPA. For each of these concentrations, electrophoresis conditions were optimized. For example, with 10µg/ml concentration, applied bias was V_{AC}=4.5V, f=10MHz produced relatively good alignment. The concentration of the CNT suspension determines numbers of CNTs between the tips, higher concentration resulting in Ohmic characteristics and lower concentrations provides good diode characteristics. Too low of a concentration (<1µg/ml) reduces the diode current and resulting in poor characteristics for THz detection.

Ohmic and Schottky Contacts: A novel process for fabricating Schottky and Ohmic contacts for a CNT Schottky diode detector is demonstrated here. This is based on the use of undercut and self-alignment approach. A simplified process flow is illustrated in Figure 7. CNTs are aligned between Ti antenna tips showing in (a), then a 150nm of another Ti is deposited by e-beam evaporation to create the Schottky contact between CNTs and Ti. Eventually, metals such as Ti (4.3eV), Al (4.06-4.26eV) and Ag (4.5eV), whose work function is smaller than that of semiconducting CNTs (4.8-4.9eV), can be used for Schottky contact. Following deposition and patterning of positive resist (step-c), Ti is selectively etched. During this step, the undercut is controlled by the type of etchant use and by the thickness of the Ti layer (150nm). The depth of undercut determines the length of the Schottky diode an in turn is small-signal model. Undercut of step-d was carried out using $HF:H_2O_2:H_2O$=1:1:200 etchant. CNTs were found to be inert to this etchant and remain semiconducting. Also, it was also determined that this etchant cleans the CNTs. After this undercut, 150nm thick gold (Au) is blanket deposited on the wafer using e-beam. The overhanging positive resist on the CNTs acts as a shadow mask. Metals such as Au (5.1-5.47eV), Pd (5.22-5.6eV) and Pt (5.12-5.93eV) whose work function is larger than that of semiconducting CNTs can be applied as Ohmic contact metals. This is followed by photo-resist lift-off of Au layer.

Patterning of this Au layer is carried out using another photoresist layer (step-g). The antenna structures, coplanar structures, and probe-pads are formed during this step. Figure 8a shows an example fabricated antenna structures. Figure 8 (b and c) also shows the Atomic Force Microscopy (AFM) pictures of the small gap formed using undercut/self-alignment process. This gap defines the effective length of the

Schottky diodes. This length can be reduced through precise control of etching rate through well controlled concentration, temperature, resist bake conditions, and uniformity of the metallization layer. AFM pictures show that the gap between the metal pads is larger than 1 μm. There are approximately 20 CNTs aligned between the Au- and Ti-pads.

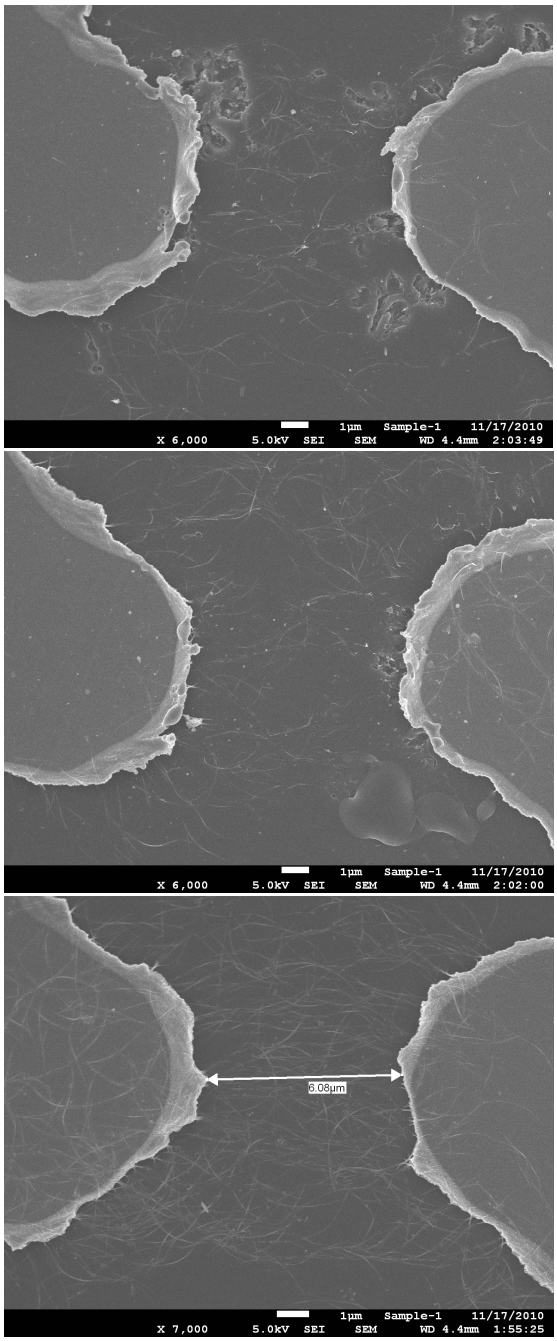

Figure 6. SEM picture of CNT alignment from three different concentrations of CNT suspended in IPA. Seen in pictures are Ti Contacts that are used in the alignment of CNTs prior to fabrication of Ohmic and Schottky contacts.

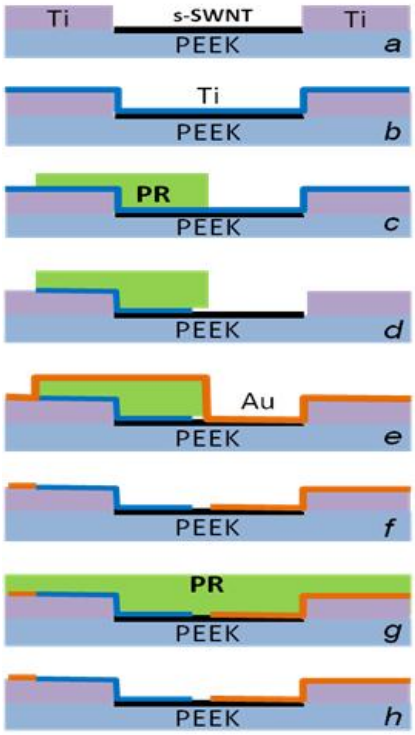

Figure 7. Forming of Ohmic and Schottky contacts on aligned CNTs. (d) shows undercut, (e) shows self-alignment.

Results: DC and Microwave Measurements

The I-V Characteristics of CNT Schottky diode detectors made from different concentrations of CNTs in IPA are shown in Figure 9. Most of the samples (Sample 1 to 5) provide a strong non-linear behavior. Here tunneling current is also involved in the contribution to the total current at higher forward bias (> 0.3 V). The reverse current has similar shape as the forward current. This indicates this is a back-to-back Schottky diode. This is because CNTs are connected with Ti on both sides. Due to the entangling of CNTs during alignment, some sample show an Ohmic behavior (sample 6), which will lead to a detector with poor performance. From these graphs, it can be stated excess concentration of CNTs should be avoided to achieve good diode performance. Decreasing the concentration will help to increase the non-linear behavior, but this also decreases the diode current and in turn increases the effective impedance of the diode and making impedance matching to antennas difficult. Thus a balance has to be reached to design an optimum diode for detector applications.

Figure 10 shows the measured I-V characteristic of a single-ended Schottky diode with Ohmic (Au) on one side and Schottky (Ti) contact on the other end. In the fabrication of this device, smaller concentrations of CNTs were used. Shown in the Figure 10 is the derivative of the I-V curve, resistance (R_s+R_d) as a function of applied voltage. This shows the diode having high effective resistance and to achieve optimum matching to antenna elements, the diode has to be operated near 1.1 V. At this voltage the effective resistance of the diode is approximately 6kΩ. Also, the non-linearity is the strongest near this bias voltage. The effective

impedance of this diode can be reduced by introducing higher concentration of CNTs in the fabrication of the device.

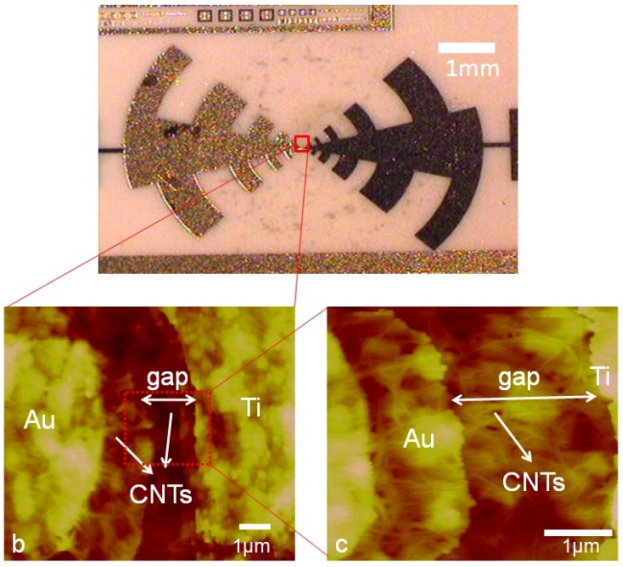

Figure 8. a) Photomicrograph of a log-periodic antenna with CNT Schottky diodes; b) AFM scan of the CNT diode region; c) Close-up view of CNT rich region.

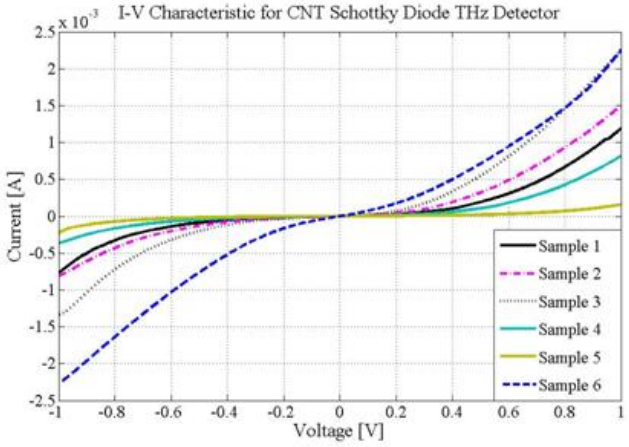

Figure 9. Measured I-V characteristics of CNT diodes with different number of CNT connected in parallel.

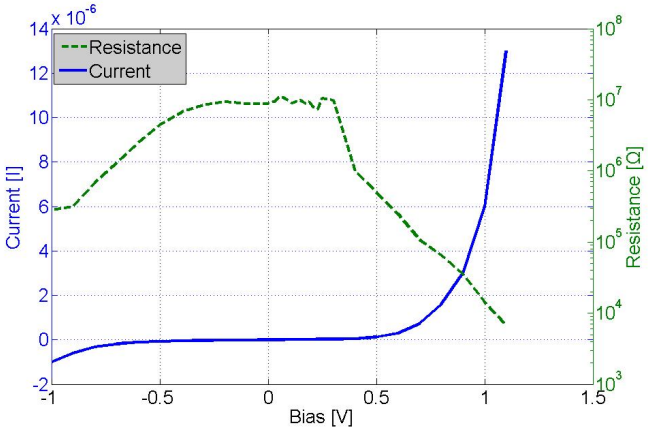

Figure 10. Measured I-V characteristics of a single-ended Schottky diode. Also shown is its derivate (effective resistance of the diode).

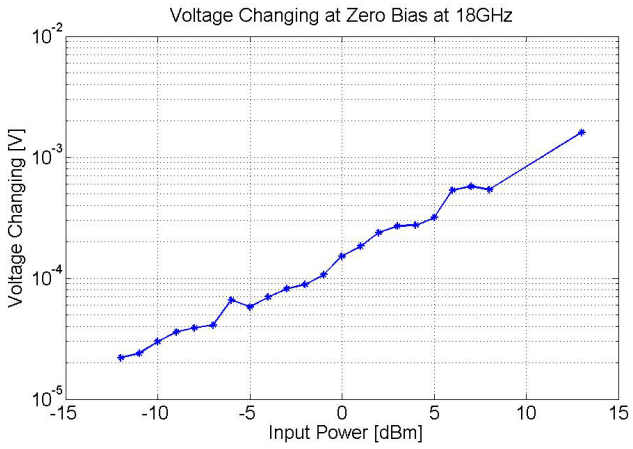

Figure 11. Measured output voltage of the diode at 18GHz as a function of power incident on the detector.

Based on the NEP calculation approach discussed earlier, the NEP value of this device was calculated for a 50Ω antenna feed. Figure 12 shows the calculated values at different frequencies. Compared to the theoretical calculations, the minimum NEP value is approximately 50pW/Hz$^{0.5}$, which is larger than what was attained from earlier simulated results. This can be attributed to poor impedance mismatch. However, these results show that good Schottky diodes can be fabricated from CNTs based on the novel process demonstrated here.

Preliminary microwave measurements of this diode were carried out using a coplanar probe setup on a probe station at 18 GHz and at zero bias. The diode is probed with a high-frequency 50Ω coplanar probe. Figure 11 shows the measured output voltage as a function of incident power onto the device. These measured results show that the detector has good sensitivity. Detailed measurements at higher frequencies using the antenna structures will be presented in the future.

Figure 13 shows the measured output voltage as a function of applied DC bias across the diode. A fixed incident power of 13dBm at 18 GHz was used in this measurement. The sensitivity increases as a function of DC bias and is highest near 0.4 V. In comparison to the plot in Figure 12, this voltage is less than the predicted voltage of approximately 0.8V. This is because the applied power of 13dBm (minus the reflected power) is significantly high and leading to self biasing of the device. Thus low bias voltage is required to achieve highest sensitivity.

Conclusions

In this paper, a novel approach to fabrication of CNT based Schottky diodes for THz detection has been demonstrated. The undercut self alignment process uses conventional microlithography approaches while achieving very small feature size. This paper shows that a large number of CNT diodes can be coupled together in parallel to achieve optimum impedance matching to antenna elements over a broad frequency range. The process allows the fabrication of CNT devices on large area low-cost substrates. A CNT diode detector was fabricated and characterized at 18 GHz using a coplanar structure. It was shown that NEP value of 50pW/Hz$^{0.5}$ at room temperature can be achieved. With impedance matching this value is expected to reach below 1pW/Hz$^{0.5}$ which is comparable with the best THz detectors

demonstrated in literature. Further measurements are being carried out at higher operating frequencies. The results of this paper will have significant impact on the development of large area compatible low-cost nanoelectronic devices for high frequency applications. Furthermore, the processing approach demonstrated here can be applied in the heterogeneous integration of CNT devices with other semiconductor technologies.

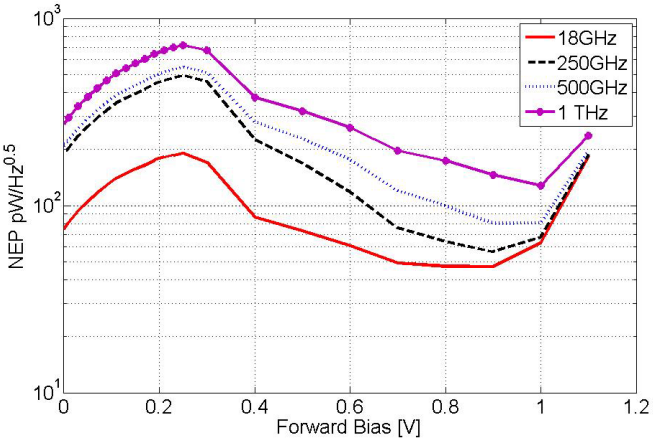

Figure 12. Calculated NEP values of the diode based on the measured I-V characteristics.

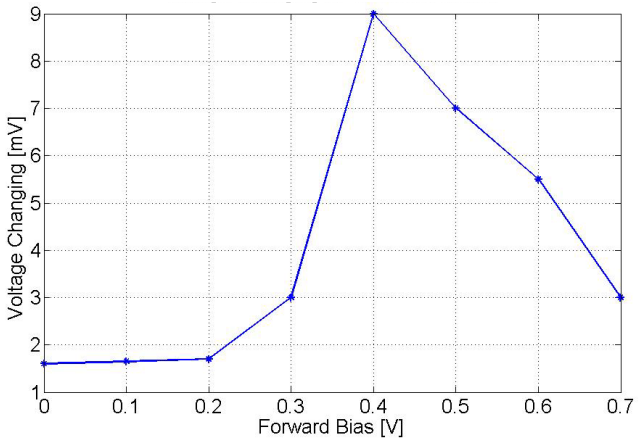

Figure 13. Measured output voltage as a function of applied voltage at a fixed incident power of 13dBm at 18 GHz. Measurement was carried out using a coplanar structure.

Acknowledgments

The authors would like to thank Dr. L. Dong's help with CNT alignment, and members of TeSLa Research Lab for helpful discussion as well as Shannon Demlow, Hongzhi Chen and Ruiguo Yang for help with the measurements. This work was partially supported by the National Science Foundation under grant ECCS1032610.

References

1. F. Sizov. et al, "Review, THz Detectors," *Progress in Quantum Electronics* Vol.34 (2010), pp. 278–347.
2. T Fuse. et al, "Quantum Response of Carbon Nanotube Quantum Dots to Terahertz Wave Irradiation," *Nanotechnology* Vol. 18 (2007), 044001 (4pp)H. M.
3. Manohara. et al. "Carbon Nanotube Schottky Diodes Using Ti-Schottky and Pt-Ohmic Contacts for High Frequency Applications," *Nano Letters* Vol. 5 (2005), No. 7, pp. 1469-1474.
4. K. Fu. et al, "Terahertz Detection in Single Wall Carbon Nanotubes," *Appl. Phys. Letter.* Vol. 92, (2008), 033105 (3pp)
5. P. Chahal, F. Morris, and G. Frazier, "Zero Bias Resonant Tunnel Schottky Contact Diode for Wide-Band Direct Detection," *IEEE Electron Device Letters*. Vol. 26, (2005), NO. 12,pp 894-896
6. J. Appenzeller. "Electronic Transport in Semi-conducting Carbon Nanotube Transistor Devices", (2003), http://nanohub.org/resources/147
7. C. Lan. et al, "Measurement of Metal/carbon Nanotube Contact Resistance by Adjusting Contact Length Using Laser Ablation," *Nanotechnology* Vol. 19 (2008) 125703 (7pp)
8. E. Cobas. et al, "Microwave Rectification by a Carbon Nanotube Schottky Diode, "*Appl. Phys. Letter*. Vol. 93, (2008), 043120, (3pp)
9. B. Shan. et al, "Ab Initio Study of Schottky Barriers at Metal-nanotube Contacts," *Physical Review B* Vol. 70, (2004), 233405 (4pp)
10. M. Budnik. et al, "A High Density Carbon Nanotube Capacitor for Decoupling Applications," *Automation Conference, 2006 43rd ACM/IEEE*, pp.935-938
11. Z. Kordrostami. et al, "Unipolar Schottky-Ohmic Carbon Nanotube Field Effect Transistor," *3rd IEEE Int. Conf. on Nano/Micro Engineered and Molecular Systems.* January 6-9, 2008, Sanya, China, pp529-531.
12. D Jimenez. et al, "A Simple Drain Current Model for Schottky-barrier Carbon Nanotube Field Effect Transistors," *Nanotechnology* Vol. 18 025201 (2007) (6pp)
13. J. M. Marulanda. et al, "Carrier Density and Effective Mass Calculations in Carbon Nanotubes," *Phys. Stat. Sol. (b)* Vol. 245, No. 11, (2008), pp2558–2562.
14. J. Hejase, P. Paladhi, and P. Chahal, "Terahertz Characterization of Dielectric Subsrates for Components Design and Non-destructive Evaluation of Packages", *IEEE Trans. On Advanced Packaging* [in review]
15. http://en.wikipedia.org/wiki/Polyethylene_terephthalate, http://en.wikipedia.org/wiki/PEEK, http://en.wikipedia.org/wiki/Polyimide.
16. Constantine A.Balanis, Antenna Theory, Analysis and Design, Wiley, (Hoboken, New Jersey, 2005), pp. 619-623.
17. D. Xu. et al, "Shaping Nanoelectrodes for High-Precision Dielectrophoretic Assembly of Carbon Nanotubes," *IEEE Transactions on Nanotechnology*. Vol. 8, NO. 4 (2009) pp.449-456.